Bibliography on Path Analysis in Functional Neuroimaging

Finn Årup Nielsen
CIMBI at DTU Informatics and NRU Rigshospitalet
Lyngby and Copenhagen, Denmark

April 23, 2010

$Revision: 1.58 $
$Date: 2008/10/23 11:28:32 $

Abstract

References for *path analysis* (structural equation modeling) and related connectivity analyses ("functional integration") for functional neuroimaging are collected.

This bibliography is part of a larger collection of bibliographies that was begun in 2001 see http://www.imm.dtu.dk/~fn/bib/Nielsen2001Bib/. The bibliography is written in LaTeX and BIB-TeX and should be available both as HTML, PDF and PostScript:

- http://www.imm.dtu.dk/~fn/bib/Nielsen2001BibPath/
- http://www.imm.dtu.dk/~fn/bib/Nielsen2001BibPath.pdf
- http://www.imm.dtu.dk/~fn/bib/Nielsen2001BibPath.ps

The bibliography is probably far from complete, but new references are added whenever the author finds new material and has the time to add them. You can email the author if corrections are required or you have found some reference that you fell ought to be included: fn@imm.dtu.dk.

Funding is from Lundbeck Foundation, the European Union project MAPAWAMO, International Neuroimaging Consortium (INC) HBM project, THOR Center for Neuroinformatics, the Villum Kann Rasmussen Foundation and the Lundbeck Foundation.

1 Terminology

Path analysis in functional neuroimaging is usually used to described the network between brain regions. In functional neuroimaging the term *structural equation modeling* (SEM) is more common. It has also been called *covariance structural equation modelling* (CSEM) (McIntosh and Gonzalez-Lima, 1994b; Taylor et al., 2000). The aspect revealed by path analysis in functional neuroimaging has been termed *effective connectivity* by Karl J. Friston, — in contrast to *functional connectivity* which describes the correlation among brain regions (Friston, 1994, 2004), cf. the related concept in spike train analysis, e.g., (Espinosa and Gerstein, 1988). *Systems-level neural modeling* has also been used to denote path analysis on the large scale brain regions (Horwitz et al., 1999, box on page 92). Analysis of the network dynamics might reveal the *transient response plasticity* (McIntosh, 2000).

2 General references

Bollen (1989, 1998b,a) gives general introductions to structural equation modeling and path analysis, and Ferron and Hess (2007) make a concrete example with maximum likelihood estimation for the structural equation model. Sánchez et al. (2005) review structural equation modeling and give an example application in environment epidemiology.

The "Computational approaches to network analysis in functional imaging" special issue of the journal *Human Brain Mapping*, volume 2, numbers 1 and 2, 1994, contains 8 contributions, e.g., (McIntosh and Gonzalez-Lima, 1994b; Gonzalez-Lima and McIntosh, 1994; Grafton et al., 1994; Friston, 1994; Alexander and Moeller, 1994; Horwitz, 1994).

Introductions to path and related analyses in functional neuroimaging are given by Büchel and Friston (1997a,b).

3 Analysis types for brain networks

If a broad angle is taken to path analysis a number of different analysis types can be regarded as "path analysis", e.g., principal component analysis (PCA), ordinary structural equation modeling, see table 1. For independent component analysis (ICA) see the *Bibliography on Independent Component Analysis in Functional Neuroimaging*, http://www.imm.dtu.dk/˜fn/bib/Nielsen2001BibICA/.

The functional connectivity can be assessed by *cross-correlation analysis between voxels*, also called "seed voxel correlation analysis". This can be done by selecting a few important voxels and examining their correlation with the rest of the brain. Worsley et al. (1998a,b, 2005a) compute the correlation from all voxels to all voxel and a threshold for on the 6D correlation random field is applied (Cao and Worsley, 1998). Worsley et al. (2005b) compare cross-correlation and SVD.

Table 1: Analysis types for brain networks

Abbrv.	Name	Comments	References
CC	Cross-correlation analysis	Cross-correlation between one region/voxel to another, also: "correlational analysis" or "seed voxel correlation analysis" (SVCA)	Metter et al. (1984b); Horwitz et al. (1984); Cao and Worsley (1998)
	Regression with PCA	Voxel-Voxel regression with principal component analysis	Friston et al. (1993)
CCA	Canonical correlation analysis		Friston et al. (1995a); Bullmore et al. (1996)
CRA	Canonical ridge analysis	Regularization of the canonical correlation analysis model so it can be perform on neuroimaging data	Nielsen et al. (1998)
PLS	Partial least squares		McIntosh and Lobaugh (2004)
PPI	Psychophysiological interaction		Friston et al. (1997)
RAM	Reticular action model		McArdle and McDonald (1984); Steele et al. (2004)
SEM	Structural equation modeling	Also called path analysis	Penny et al. (2004)
RD	Replicator dynamics		Lohmann and Bohn (2002)
SVD	Singular value decomposition	Similar to principal component analysis	Sychra et al. (1994): On fMRI
SSM	Scaled subprofile model		Moeller et al. (1987)
DCM	Dynamic Causal Modeling		Friston et al. (2003); Friston (2003); Penny et al. (2004)

The validity of the inference made by dynamic causal modeling is explored by Lee et al. (2006).

3.1 Mathematical description of structural equations model

A general form of structural equations is (Bollen, 1989, eqs. 2.4, 2.8 and 2.9):

$$\mathbf{N} = \mathbf{N}\mathbf{B} + \mathbf{\Xi}\mathbf{\Gamma} + \mathbf{Z} \tag{1}$$
$$\mathbf{X} = \mathbf{\Xi}\mathbf{\Lambda}_x + \mathbf{\Delta} \tag{2}$$
$$\mathbf{Y} = \mathbf{N}\mathbf{\Lambda}_y + \mathbf{E} \tag{3}$$

The first equation is for the latent variables, while the second and third equations ("the measurement model") relate the latent variables to the observed variables, $\mathbf{X}$ and $\mathbf{Y}$. The diagonal of $\mathbf{B}$ should be zero.

If there is no measurement noise, $\mathbf{\Delta} = \mathbf{0}$ and $\mathbf{E} = \mathbf{0}$, and there is a one-to-one relationship between the latent and observed variables, $\mathbf{\Lambda}_x = \mathbf{I}$ and $\mathbf{\Lambda}_y = \mathbf{I}$, then the structural equations can be written as

$$\mathbf{Y} = \mathbf{Y}\mathbf{B} + \mathbf{X}\mathbf{\Gamma} + \mathbf{Z} \tag{4}$$

In econometrics one finds the so-called "structural form" in "simultaneous equation systems" (Mardia et al., 1979, section 7.3, equation 7.3.1)

$$\mathbf{Y}\mathbf{B} + \mathbf{X}\mathbf{\Gamma} = \mathbf{U} \tag{5}$$

This is equivalent to equation 4 with suitable redefinitions, e.g., $\mathbf{B} \to \mathbf{I} - \mathbf{B}$, $\mathbf{\Gamma} \to -\mathbf{\Gamma}$ and $\mathbf{Z} \to \mathbf{U}$.

$\mathbf{\Xi}$ and $\mathbf{X}$ are called the *exogenous* or independent variables while $\mathbf{N}$ and $\mathbf{Y}$ are called the *endogenous* variables. If there are no exogenous variables, $\mathbf{X} = \mathbf{0}$, then equation 4 simplifies to

$$\mathbf{Y} = \mathbf{Y}\mathbf{B} + \mathbf{Z} \tag{6}$$

When regarding this equation as a network the columns of the $\mathbf{Y}$ are the nodes of the network, while the $\mathbf{B}$ matrix describes the links between the nodes.

3.1.1 Functional neuroimaging

Functional neuroimaging tends to use the relatively simple equation 6, though, e.g., with this renaming

$$\mathbf{X} = \mathbf{X}\mathbf{K} + \mathbf{U} \tag{7}$$

Most often $\mathbf{X}(N \times P)$ will contain data from brain scannings, e.g., as a $\mathbf{X}(\text{scans} \times \text{brain regions})$ matrix, while $\mathbf{K}(\text{brain regions} \times \text{brain regions})$ is the "network" one wants to estimate and this is typically regarded as sparse, i.e., many elements are zero.

An example taken from (Bullmore et al., 2000, page 295) with a transposed notation for a single scan

$$\mathbf{x}_{(n)}^{\mathsf{T}} = \mathbf{K}^{\mathsf{T}}\mathbf{x}_{(n)}^{\mathsf{T}} + \mathbf{u}_{(n)}^{\mathsf{T}} \tag{8}$$

$$\begin{bmatrix} \text{VEC} \\ \text{PFC} \\ \text{SMA} \\ \text{IFG} \\ \text{IPL} \end{bmatrix} = \begin{bmatrix} 0 & 0 & 0 & 0 & \theta_1 \\ \theta_2 & 0 & 0 & 0 & 0 \\ 0 & \theta_3 & 0 & 0 & 0 \\ 0 & 0 & \theta_4 & 0 & 0 \\ \theta_6 & 0 & 0 & \theta_5 & 0 \end{bmatrix} \times \begin{bmatrix} \text{VEC} \\ \text{PFC} \\ \text{SMA} \\ \text{IFG} \\ \text{IPL} \end{bmatrix} + \begin{bmatrix} \psi_1 \\ \psi_2 \\ \psi_3 \\ \psi_4 \\ \psi_5 \end{bmatrix} \tag{9}$$

In this kind of application of structural equation modeling the brain regions are the nodes of the network. Multisubject extension to this scheme make nodes also over subject so the matrix $\mathbf{X}$ gets the size $(\text{scans} \times (\text{brain regions} \times \text{subjects})\,)$ (Mechelli et al., 2002).

3.1.2 Number of networks

The number of different networks (in terms of zero structure) for even small sized structure matrices is very large. For a two-by-two structure matrix, $\mathbf{K}(2 \times 2)$, there are 3 non-zero networks and 4 if we allow for the zero network: There are two elements of the structure matrix that can either by zero or non-zero independent of each other. This gives all compinations: $2^2 = 4$. Generally, for a N-by-N structure matrix, $\mathbf{K}(N \times N)$, the form for the number of networks $L(N)$ is:

$$L(N) = 2^{N \times N - N} = 2^{N(N-1)} \tag{10}$$

Some examples: $L(3) = 64$, $L(4) = 4\,096$, $L(5) = 1\,048\,576$, $L(6) = 1\,073\,741\,824$.

If one considers a growing network where one non-zero element in the structure matrix is added at a time, and when a non-zero element is added it is maintained in the network, then the number of possible networks shrinks dramatically. The number of possible non-zero elements to start with is $M = N(N-1)$. When the first element is added and the network is incremented with a new non-zero element then there are $M-1$ elements left to choose from. In the next step only $M-2$ and so on until the all off-diagonal element of the structure matrix is non-zero. The form for the total number of networks that is traversed is

$$L_{\text{grow}}(N) = \sum_{m=0}^{M} (M-m) = M(M+1) - \frac{M(M+1)}{2} = \frac{M(M+1)}{2} \tag{11}$$

$$= \frac{N(N-1)\,(N(N-1)+1)}{2} = \frac{N^4 - 2N^3 + 2N^2 - N}{2} \tag{12}$$

Some examples: $L_{\text{grow}}(2) = 3$, $L_{\text{grow}}(3) = 21$, $L_{\text{grow}}(4) = 78$, $L_{\text{grow}}(5) = 210$, $L_{\text{grow}}(6) = 465$ and $L_{\text{grow}}(7) = 903$.

3.2 Other remarks

Panel analysis is a dynamic (longitudinal) form of path analysis, see, e.g., Easdon and McIntosh (2000) for an application in functional neuroimaging. Büchel et al. (1999) investigated the change in path coefficients over time in associative learning.

Structural equation modeling on BOLD fMRI may be confounded by 1/f-noise and/or cardiac and respiratory noise that can cause nuisance connectivity, see, e.g., a comment by Lund (2001).

3.3 Tools

Some of the few tools that enable path and related analyses are listed in in table 2. Haughton et al. (2006) describes three software packages for directed acyclic graphs: MIM, Tetrad and WinMine.

Table 2: Analysis types for brain networks.

Name	Description	References
gR	Graphical modeling in R	
LiNGAM	"Discovery of non-gaussian linear causal models" matlab programs	Shimizu et al. (2006), http://www.cs.helsinki.fi-/group/neuroinf/lingam/
MIM		Edwards (2000, 1995), http://www.hypergraph.dk,
Mplus	Commercial windows program for structural equations modeling	Muthén and Muthén (2006), http://www.statmodel.com/
Mx	Binary programs for Linux, Mac, Unix and Windows	Neale et al. (2003), http://www.vcu.edu/mx/
SEM (Steele)	Structural equation modeling implemented in Matlab by J. Douglas Steele	http://www.abdn.ac.uk/~men204/SEM.htm
SPM2 DCM	Dynamic Causal Modeling as implemented in SPM2	Friston et al. (2003); Friston (2003)
LISREL	Commercial general structural equation modeling program	http://www.ssicentral.com/other/entry.htm

Name	Description	References

4 Applications

Some early examples: Høedt-Rasmussen and Skinhøj (1964) compared hemispheric cerebral blood flow based on measurements with Krypton-85. Paulson (1970); Paulson et al. (1970) compute the "interchannel coefficient of variation" (or "interregional coefficient of variation") between 16 channels measuring cerebral blood flow with Xenon-133.

Most studies analyze functional brain scans. However, there has also been a study that considered the covariance between gray matter density in different brain regions via voxel-based morphometry (Mechelli et al., 2005). .

Table 3: Path analyses in functional neuroimaging. VEC: ventral extrastriate cortex, PFC: prefrontal cortex, SMA: supplementary motor area, IFG: Interior frontal gyrus, IPL: Inferior parietal lobule.

Type	Scan	Variables-/Regions	Behavioral domain	Remarks	Reference
		—	—	Review	McIntosh (1999)
					Horwitz et al. (1999)
		—	—	Review	Taylor et al. (2000)
—	—	—	Overview	Brief describtion in section 3.1	Horwitz et al. (2000a)
CC	PET	$2 \times 23 + 3$	Resting	Partial correlation, kappa statistics	Horwitz et al. (1984)
CC	PET	2×?	Normals		Metter et al. (1984b)
CC	PET	2×?	Resting	Normals, Alzheimer, Huntington, Parkinson	Metter et al. (1984a)
SEM	PET	2×7: BA 17/18, 19d, 19v, 7, 37, 21, 46	Object and spatial vision		McIntosh and Gonzalez-Lima (1994b); McIntosh et al. (1994)
?	?	?	?	?	Horwitz (1994)
SEM	PET	5: SMA/cing, motor, putamen, GP, thalamus	Movement	Controls and Parkinson's disease patients	Grafton et al. (1994)
CC	fMRI		Vision		Kleinschmidt et al. (1994)
CC	fMRI	?	Resting state		Biswal et al. (1995)
SEM	PET	?	Face matching with Alzheimer patients		Horwitz et al. (1995)
CC/SEM	PET	11 regions	reading, visual word recognition		Nyberg et al. (1996)

Type	Scan	Variables-/Regions	Behavioral domain	Remarks	Reference
SEM	fMRI	?	Visual motion	Modulation modeled with interaction term	Büchel and Friston (1997c)
?	PET	?	Semantic processing in schizophrenia		Jennings et al. (1998)
CC	PET		Reading and dyslexia		Horwitz et al. (1998)
CC	PET	All voxels	Vigilance task	Correlation field threshold via random field theory	Worsley et al. (1998a,b)
SEM	fMRI	2 × 7	Motor task	Low-frequency BOLD fMRI	Lowe (1999)
?	PET	?	Face encoding and recognition		Rajah et al. (1999)
?	PET	?	Episodic encoding and retrieval of words		Krause et al. (1999)
?	fMRI	?	Associative learning		Büchel et al. (1999)
CC	fMRI	A few voxels in hippocambus and thalamus	Resting state		Stein et al. (2000)
?	PET		Language processing		Petersson et al. (2000)
CC	PET	Wernicke, Broca, others	Language production		Horwitz et al. (2000b)
CC	fMRI	Voxels in Rolandic cortex, ventrolateral thalamus, anterior putamen correlated with the rest of the brain	Motor		Mopritz et al. (2000)
Panel/PLS	PET	Left cerebellum, left superior fronal cortex	Eyeblink conditioning		Easdon and McIntosh (2000)
PLS	PET		Short-term memory wrt. age		Della-Maggiore et al. (2000)
SEM	fMRI	5: VEC, PFC, SMA, IFG, IPL	Semantic decision, subvocal rehearsal	Model order determination by P-values, AIC and Bollen's "parsimonious fit index"	Bullmore et al. (2000)
SEM	fMRI	7	Memory retrieval		Maguire et al. (2000)
SEM	PET	?	?		Nezafat et al. (2001)

Type	Scan	Variables-/Regions	Behavioral domain	Remarks	Reference
CC	fMRI	From/to anterior cerebellum	Simple motor task	Schizophrenia and control subjects	Stephan et al. (2001)
?	fMRI	9: EC, BA37, IPS, SMA, FEF, VPC, IFG, PSTS, AG	Implicit language processing		?
SEM	PET	12	Working memory	Split-half validation, AIC and RMSEA	Glabus et al. (2003)
PLS	?	39		FDG, rats,	Nair and Gonzalez-Lima (2003)
SEM	fMRI	10	Visual attention	In normals and Williams syndrome	Meyer-Lindenberg et al. (2004)
RAM	fMRI	5	Predictive error signal	Depressive illness	Steele et al. (2004)
CC	fMRI	Voxels	Finger opposition	Power law, clustering coefficient and path length computed (small world variables)	Eguíluz et al. (2005)
SEM	fMRI	10	Flanker task (attentional control)		Erickson et al. (2005)
SEM	fMRI	4	Emotional face processing	In normals and Williams syndrome	Meyer-Lindenberg et al. (2005)
SEM	fMRI	8 regions around amygdala	Negative emotional faces	Minimization with adaptive simulated annealing and with split half verification	Stein et al. (2006)
CC	fMRI	90 regions	Resting state with pharmacological stimulation	Wavelet correlation analysis in the frequency interval 0.06–0.11 and with metrics of network efficiency (small world	Achard and Bullmore (2007)
SEM	MRI		None	Size of brain regions	Colibazzi et al. (2008)

4.1 Resting state path analysis

Functional connectivity has been assessed with resting state BOLD fMRI (Biswal et al., 1995), e.g., Stein et al. (2000) pick a few seed voxels in the thalamus and the hippocambus and compute the correlation coefficient between these (each at a time) and the rest of the brain, thresholding at 0.5. The correlation is high for low frequencies (< 0.1 Hz), and hypercapnia results in a substantial decrease in the correlation (Biswal et al., 1997). Lowe et al. (1998) report low-frequency resting state fluctuation with low sampling rate multislice. Xiong et al. (1999) pick the seed in the primary motor cortex.

4.2 Unclassified

Kim et al. (2007): MAR, SEM, GLM

Clark et al. (1984)

Koch et al. (2002): Comparison of functional and anatomical connectivity.

McIntosh and Gonzalez-Lima (1991): SEM on auditory system.

McIntosh and Gonzalez-Lima (1992): SEM on the visual system of the rat.

McIntosh and Gonzalez-Lima (1994a)

Anatomically based structural equation modeling (SEM) Rajah et al. (1999)

Friston et al. (1995b) "regression".

Cordes et al. (2001)

(Büchel and Friston (1998): "variable parameter regression" and Kalman filtering)

Cordes 2000, AJNR, 21:1636

4.2.1 "Structural equation" and PET

From PubMed: Nezafat et al. (2001), Della-Maggiore et al. (2000), Petersson et al. (2000), Taylor et al. (2000), McIntosh (1999), Rajah et al. (1999), Horwitz et al. (1999), McIntosh (1998), Jennings et al. (1998), Cabeza et al. (1997), McIntosh et al. (1994).

5 Other connectivity analyses

Brain connectivity may also be obtained from tractography of diffusion spectrum imaging (Hagmann et al., 2008).

A Examples of networks

A.1 Object and spatial vision

The following functional networks are originally from McIntosh et al. (1994). The network descriptions are in the *dot* file format Koutsofios and North (1996) and figures 1 and 2 display the output from the program. Negative path coefficients are indicated by dotted lines.

```
digraph ObjectVision {
    rankdir=LR
    "17/18" -> "19v"
    "17/18" -> "19d" [style=dotted]
    "19v" -> "37"
    "19v" -> "19d"
    "19d" -> "7" [style=dotted]
    "19d" -> "46" [style=dotted]
    "37" -> "21"
    "37" -> "7" [style=dotted]
    "7" -> "21"
    "7" -> "46" [style=dotted]
    "21" -> "46"
    "46" -> "19v" [style=dotted]
}

digraph SpatialVision {
    rankdir=LR
    "17/18" -> "19v"
    "17/18" -> "19d"
    "19v" -> "37"
    "19v" -> "19d"
    "19d" -> "7"
```

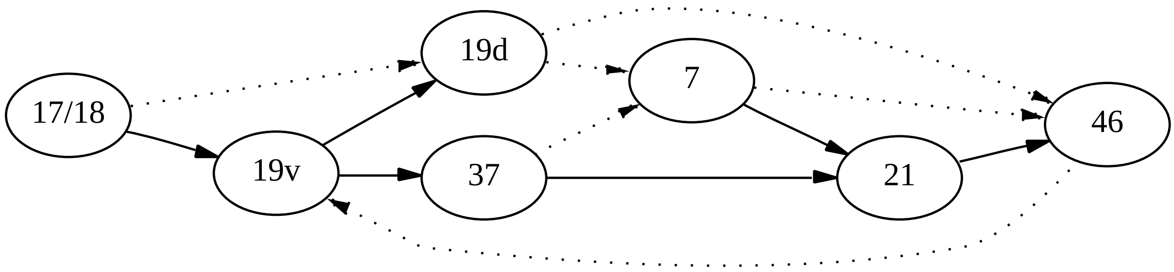

Figure 1: Object vision functional network for the right hemisphere. Adapted from (Horwitz, 1994, figure 3) which is adapted from McIntosh et al. (1994).

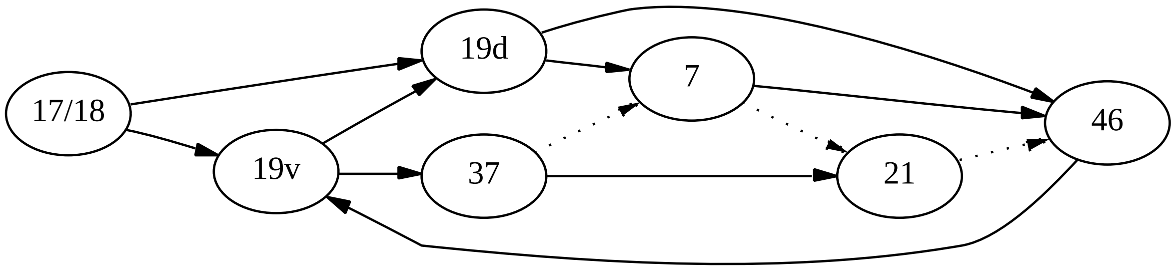

Figure 2: Spatial vision functional network for the right hemisphere. Adapted from (Horwitz, 1994, figure 3) which is adapted from McIntosh et al. (1994).

```
    "19d" -> "46"
    "37" -> "21"
    "37" -> "7" [style=dotted]
    "7" -> "21" [style=dotted]
    "7" -> "46"
    "21" -> "46" [style=dotted]
    "46" -> "19v"
}
```

McIntosh and Gonzalez-Lima (1994b) consider interhemispheric functional models for the same task.

A.2 Motor system

Motor system connectivity is examined by Grafton et al. (1994) who used a cortical-subcortical network proposed by Alexander et al. (1990); DeLong (1990). Some of the results from a LISREL estimation are displayed in figure 3 and the corresponding *dot* file is shown below.

```
digraph GraftonS1994Network {
        subgraph clusterNormalMovement {
                label="Normal subjects, Movement task";
                ranksep=0.75;
                { rank = same;
                        NM1 [label="SMA & Cingulate\n Motor Areas" ];
                        NM2 [label="Motor cortex"];
```

```
		}
		NM3 [label="Putamen"]
		{ rank = same;
			NM4 [label="Globus pallidus"];
			NM5 [label="Ventrolateral\n Thalamus"];
		}
		NM1 -> NM2
		NM1 -> NM3 [style=dotted]
		NM1 -> NM5
		NM2 -> NM3 [style=dotted]
		NM2 -> NM5 [style=dotted]
		NM3 -> NM4
		NM4 -> NM5
		NM5 -> NM1
		NM5 -> NM2 [style=dotted]
	}
	subgraph clusterParkinsonBefore {
		label="Parkinson patients, before pallidotomy";
		ranksep=0.75;
		{ rank = same;
			PB1 [label="SMA & Cingulate\n Motor Areas" ];
			PB2 [label="Motor cortex"];
		}
		PB3 [label="Putamen"]
		{ rank = same;
			PB4 [label="Globus pallidus"];
			PB5 [label="Ventrolateral\n Thalamus"];
		}
		PB1 -> PB2
		PB1 -> PB3 [style=dotted]
		PB1 -> PB5
		PB2 -> PB3
		PB2 -> PB5
		PB3 -> PB4
		PB4 -> PB5
		PB5 -> PB1
		PB5 -> PB2
	}
}
```

A.3 Cognition

A visual implicit language processing network:

```
digraph McKiernanK2001Development {
    rankdir=LR
    IFG -> VPC
    SMA -> VPC
    FEF -> SMA
    FEF -> VPC
    FEF -> IPC
    PSTS -> IFG
    PSTS -> FEF
    PSTS -> AG
    AG -> IFG [style=dotted]
    IPS -> IFG
```

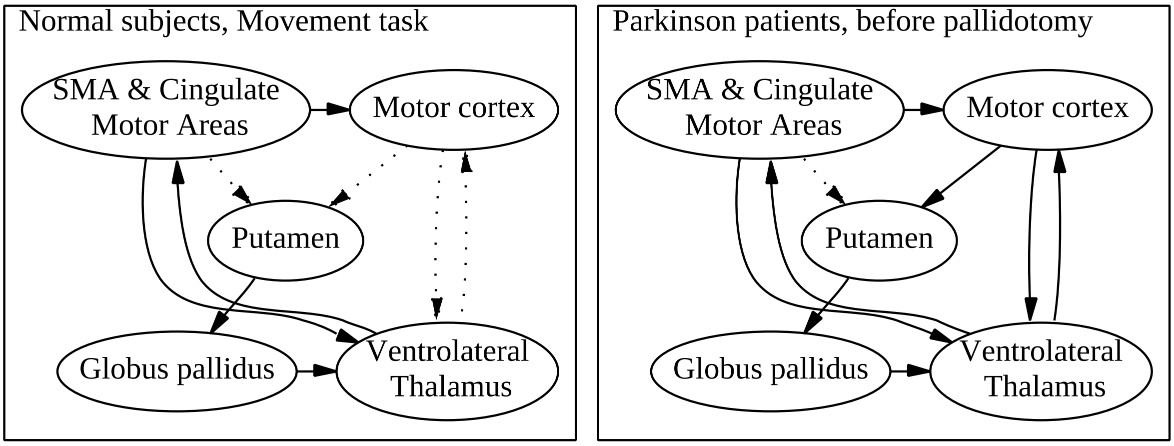

Figure 3: Movement network from Grafton et al. (1994).

```
    IPS -> VPC
    IPS -> AG
    BA37 -> PSTS
    BA37 -> VPC [style=dotted]
    BA37 -> IPS
    EC -> BA37
}
```

References

Achard, S. and Bullmore, E. (2007). Efficiency and cost of economical brain functional networks. *PLoS Computational Biology*, 3(2):e17. DOI: 10.1371/journal.pcbi.0030017.

Alexander, G. E., Crutcher, M. D., and DeLong, M. R. (1990). Basal ganglia thalamo-cortical circuits: Parallel substrates for motor, oculomotor, “prefrontal” and “limbic” functions. *Prog. Brain Res.*, 85:119–146.

Alexander, G. E. and Moeller, J. R. (1994). Application of the scaled subprofile model to functional imaging in neuropsychiatric disorders: A principal component approach to modeling brain function in disease. *Human Brain Mapping*, 2(1 and 2):79–94. ISSN 1065-9471.

Biswal, B., Hudetz, A. G., Yetkin, F. Z., Haughton, V. M., and Hyde, J. S. (1997). Hypercapnia reversibly suppresses low-frequency fluctuations in the human motor cortex during rest using echo-planar MRI. *Journal of Cerebral Blood Flow and Metabolism*, 17(3):301–308. PMID: 9119903.

Biswal, B., Yetkin, F. Z., Haughton, V. M., and Hyde, J. S. (1995). Functional connectivity in the motor cortex of resting human brain using echo-planar MRI. *Magnetic Resonance in Medicine*, 34(4):537–541. PMID: 8524021. ISSN 0740-3194.

Bollen, K. A. (1989). *Structural Equations with Latent Variables*. Wiley Series in Probability and Mathematical Statistics. John Wiley & Sons, New York.

Bollen, K. A. (1998a). Path analysis. In Armitage, P. and Colton, T., editors, *Encyclopedia of biostatistics*, pages 3280–3284. John Wiley & Sons, West Sussex, England. ISBN 0471975761.

Bollen, K. A. (1998b). Structural equation models. In Armitage, P. and Colton, T., editors, *Encyclopedia of biostatistics*, pages 4363–4372. John Wiley & Sons, West Sussex, England. ISBN 0471975761.

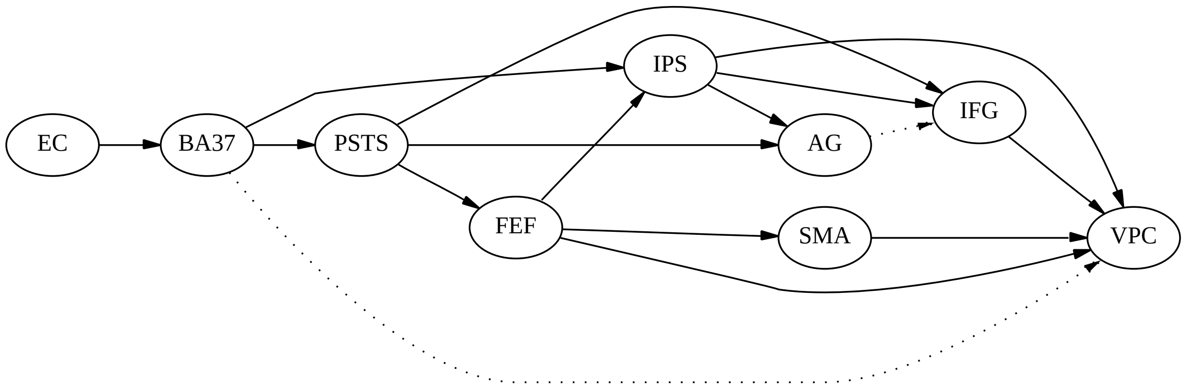

Figure 4: Visual implicit language processing McKiernan et al. (2001).

Büchel, C., Coull, J. T., and Friston, K. J. (1999). The predictive value of changes in effective connectivity for human learning. *Science*, 283(5407):1538–1541. PMID: 10066177. ISSN 0036-8075.

Büchel, C. and Friston, K. J. (1997a). Characterising functional integration. In Frackowiak, R. S. J., Friston, K. J., Frith, C. D., Dolan, R. J., and Mazziotta, J. C., editors, *Human Brain Function*, chapter 7, pages 127–140. Academic Press, San Diego, California.

Büchel, C. and Friston, K. J. (1997b). Effective connectivity and neuroimaging. In *SPMcourse, short course notes*, chapter 6. Institute of Neurology, Wellcome Department of Cognitive Neurology, London, UK. http://www.fil.ion.ucl.ac.uk/spm/course/notes97/Ch6.pdf.

Büchel, C. and Friston, K. J. (1997c). Modulation of connectivity in visual pathways by attention: cortical interactions evaluated with structural equation modelling and fMRI. *Cerebral Cortex*, 7(8):768–778. PMID: 9408041.

Büchel, C. and Friston, K. J. (1998). Dynamic changes in effective connectivity characterized by variable parameter regression and Kalman filtering. *Human Brain Mapping*, 6(5–6):403–408. ISSN 1065-9471.

Bullmore, E., Horwitz, B., Honey, G., Brammer, M., Williams, S., and Sharma, T. (2000). How good is good enough in path analysis of fMRI data? *NeuroImage*, 11(4):289–301. PMID: 10725185. http://www-staff.psychiatry.cam.ac.uk/~gh242/Bullmore_Neuroimage_(11)_2000.pdf. Path analysis with fMRI data on five brain regions with model order determination through P-values, Akaike's AIC and Bollen's parsimonous fit index.

Bullmore, E. T., Rabe-Hesketh, S., Morris, R. G., Williams, S. C. R., and Gregory, L. (1996). Functional magnetic resonance image analysis of a large-scale neurocognitive network. *NeuroImage*, 4(1):16–33. PMID: 9345494. DOI: 10.1006/nimg.1996.0026. WOBIB: 113. http://www.sciencedirect.com/science/article/B6WNP-45MGVH0-1P/2/33287689eb5bee8ad10fe7df7535d969. ISSN 1053-8119.

Cabeza, R., McIntosh, A. R., Tulving, E., Nyberg, L., and Grady, C. L. (1997). Age-related differences in effective neural connectivity during encoding and recall. *NeuroReport*, 8(16):3479–3483. PMID: 9427311.

Cao, J. and Worsley, K. J. (1998). The geometry of correlation fields with an application to functional connectivity of the brain. *Annals of Applied Probability*, 9:1021–1057. http://www.math.mcgill.ca/~keith/correl/correl.abstract.html.

Clark, C. M., Kessler, R., Buchsbaum, M. S., Margolin, R. A., and Holcomb, H. H. (1984). Correlational methods for determining regional coupling of cerebral glucose metabolism: a pilot study. *Biological Psychiatry*, 19(5):663–678.

Colibazzi, T., Zhu, H., Bansal, R., Schultz, R. T., Wang, Z., and Peterson, B. S. (2008). Latent volumetric structure of the human brain: Exploratory factor analysis and structural equation modeling of gray matter volumes in healthy children and adults. *Human Brain Mapping*, 29(11):1302–1312. DOI: 10.1002/hbm.20466.

Cordes, D., Haughton, V., Arfanakis, K., Carew, J., and Turski, P. (2001). Decomposition of cross correlation maps into frequency components to measure functional connectivity in resting state MRI data. *NeuroImage*, 13(6):S99.

Della-Maggiore, V., Sekuler, A. B., Grady, C. L., Bennett, P. J., Sekuler, R., and McIntosh, A. R. (2000). Corticolimbic interactions associated with performance on a short-term memory task are modified by age. *Journal of Neuroscience*, 20(22):8410–8416. PMID: 11069948.

DeLong, M. R. (1990). Primate models of movement disorders of basal ganglia origin. *Trends in Neurosciences*, 13(281–285).

Easdon, C. and McIntosh, A. R. (2000). Measuring dynamic connectivity in eyeblink conditioning: A panel analysis. *NeuroImage*, 11(5, part 2):S572. Sixth Annual Meeting of the Organization For Human Brain Mapping.

Edwards, D. (1995). *Introduction to Graphical Modelling*. Springer texts in statistics. Springer Verlag, Heidelberg. ISBN 0387944834.

Edwards, D. (2000). *Introduction to graphical modelling*. Springer texts in statistics. Springer. ISBN 0387950540.

Eguíluz, V. M., Chialvo, D. R., Cecchi, G. A., Baliki, M., and Apkarian, A. V. (2005). Scale-free brain functional networks. *Physical Review Letters*, 94(018102):1–4. http://link.aps.org/abstract/PRL/v94/e018102.

Erickson, K. I., Ho, M.-H. R., Colcomb, S. J., and Kramer, A. F. (2005). A structural equation modeling analysis of attentional control: an event-related fMRI study. *Cognitive Brain Research*, 22:349–357. DOI: 10.1016/j.cogbrainres.2004.09.004.

Espinosa, I. E. and Gerstein, G. L. (1988). Cortical auditory neuron interactions during presentation of 3-tone sequences: effective connectivity. *Brain Research*, 450(1–2):39–50. PMID: 3401720.

Ferron, J. M. and Hess, M. R. (2007). Estimation in SEM: A concrete example. *Journal of Educational and Behavioral Statistics*, 32(1):110–120. DOI: 10.3102/1076998606298025.

Friston, K. J. (1994). Functional and effective connectivity in neuroimaging: A synthesis. *Human Brain Mapping*, 2(1 and 2):56–78. DOI: 10.1002/hbm.460020107. http://www3.interscience.wiley.com/cgi-bin/fulltext/109711709/PDFSTART. ISSN 1065-9471.

Friston, K. J. (2003). Dynamical causal models. In Frackowiak, R. S. J., Friston, K. J., Dolan, R., and Price, C., editors, *Human Brain Function*, chapter 22. Academic Press, second edition. http://www.fil.ion.ucl.ac.uk/spm/HBF2/pdfs/Ch22.pdf. ISBN 0122648412.

Friston, K. J. (2004). Functional integration in the brain. In Frackowiak, R. S. J., Friston, K. J., Frith, C. D., Dolan, R. J., Price, C. J., Zeki, S., Ashburner, J., and Penny, W., editors, *Human Brain Function*, chapter 48, pages 971–997. Elsevier, Amsterdam, Holland, second edition. http://www.fil.ion.ucl.ac.uk/spm/doc/books/hbf2/pdfs/Ch18.pdf.

Friston, K. J., Büchel, C., Fink, G. R., Morris, J., Rolls, E., and Dolan, R. J. (1997). Psychophysiological and modulatory interactions in neuroimaging. *NeuroImage*, 6(3):218–229. PMID: 9344826. http://www.fil.ion.ucl.ac.uk/spm/doc/papers/karl_ppi.pdf.

Friston, K. J., Frith, C. D., and Frackowiak, R. S. J. (1993). Time-dependent changes in effective connectivity measured with PET. *Human Brain Mapping*, 1(1):69–80. DOI: 10.1002/hbm.460010108. Presents a model with regression from voxels to voxels by first performing a principal component analysis on the neuroimaging data and then estimate the regression parameters from the principal components to the neuroimaging data.

Friston, K. J., Frith, C. D., Frackowiak, R. S. J., and Turner, R. (1995a). Characterizing dynamic brain responses with fMRI: A multivariate approach. *NeuroImage*, 2(2):166–172. DOI: 10.1006/nimg.1995.1019. http://www.fil.ion.ucl.ac.uk/spm/doc/papers-/karl_dyn_multivariate.pdf.

Friston, K. J., Harrison, L., and Penny, W. (2003). Dynamic causal modelling. *NeuroImage*, 19(4):1273–1302. PMID: 12948688.

Friston, K. J., Ungeleider, L. G., Jezzard, P., and Turner, R. (1995b). Characterizing modulatory interactions between V1 and V2 in human cortex with fMRI. *Human Brain Mapping*, 2:211–224.

Glabus, M. F., Horwitz, B., Holt, J. L., Kohn, P. D., Gerton, B. K., Callicott, J. H., Meyer-Lindenberg, A., and Berman, K. F. (2003). Interindividual differences in functional interactions among prefrontal, parietal and parahippocampal regions during working memory. *Cerebral Cortex*, 13(12):1352–1361. PMID: 14615300. DOI: 10.1093/cercor/bhg082. Structural equations modeling of PET images with normal subjects performing a working memory task. The MX software was used with AIC and root-means quare error of approximation and a split-half validation. Talairach coordinates and path coefficients are reported.

Gonzalez-Lima, F. and McIntosh, A. R. (1994). Neural network interactions related to auditory learning analyzed with structural equation modeling. *Human Brain Mapping*, 2(1 and 2):23–44. ISSN 1065-9471.

Grafton, S. T., Sutton, J., Couldwell, W., Lew, M., and Waters, C. (1994). Network analysis of motor system connectivity in parkinson's disease: Modulation of thalamocortical interactions after pallidotomy. *Human Brain Mapping*, 2(1 and 2):45–55. ISSN 1065-9471.

Hagmann, P., Cammoun, L., Gigandet, X., Meuli, R., Honey, C. J., and Wedeen, V. J. (2008). Mapping the structural core of human cerebral cortex. *PLoS Biology*, 6(7):e157. DOI: 10.1371/journal.pbio.0060159.

Haughton, D., Kamis, A., and Scholten, P. (2006). A review of three directed acyclic graphs software packages: MIM, Tetrad, and WinMine. *The American Statistician*, 60(3):272–286. DOI: 10.1198/000313006X117972.

Høedt-Rasmussen, K. and Skinhøj, E. (1964). Transneural depression of the cerebral hemispheric metabolism in man. *Acta Neurologica Scandinavica*, 40:41–46. 2-channel measurements of regional cerebral blood flow with Krypton-85. The measurements are compared between the hemispheres.

Horwitz, B. (1994). Data analysis paradigms for metabolic-flow data: through the skull: Advanced EEGs use MRIs to accurately measure combining neural modeling and functional neuroimaging. *Human Brain Mapping*, 2(1 and 2):112–122. ISSN 1065-9471.

Horwitz, B., Duara, R., and Rapoport, S. I. (1984). Intercorrelations of glucose metabolic rates between brain regions: Application to healthy males in a state of reduced sensory input. *Journal of Cerebral Blood Flow and Metabolism*, 4(4):484–499. ISSN 0271-678X.

Horwitz, B., Friston, K. J., and Taylor, J. G. (2000a). Neural modeling and functional brain imaging: an overview. *Neural Networks*, 13(8–9):829–846. PMID: 11156195. http://www.ling.umd.edu/poeppel/HorwitzPET.pdf.

Horwitz, B., Jeffries, K. J., and Braun, A. R. (2000b). Functional connectivity among language areas during speech production. In Fox, P. T. and Lancaster, J. L., editors, *Sixth International Conference on Functional Mapping of the Human Brain, NeuroImage*, volume 11, page S284. Academic Press. ISSN 1053-8119. Demonstrates varying cross-correlation among Wenicke's and Broca's during different language production tasks.

Horwitz, B., McIntosh, A. R., Haxby, J. V., Furey, M., Salerno, J. A., Schapiro, M. B., Rapoport, S. I., and Grady, C. L. (1995). Network analysis of PET-mapped visual pathways in Alzheimer type dementia. *NeuroReport*, 6(17):2287–2292. PMID: 8747138.

Horwitz, B., Rumsey, J. M., and Donohue, B. C. (1998). Functional connectivity of the angular gyrus in normal reading and dyslexia. *Proceedings of the National Academy of Sciences*, 95(15):8939–8944.

Horwitz, B., Tagamets, M. A., and McIntosh, A. R. (1999). Neural modeling, functional brain imaging, and cognition. *Trends in Cognitive Science*, 3(3):91–98. PMID: 10322460.

Jennings, J. M., McIntosh, A. R., Kapur, S., Zipursky, R. B., and Houle, S. (1998). Functional network differences in schizophrenia: a rCBF study of semantic processing. *NeuroReport*, 9(8):1697–1700. PMID: 9665585.

Kim, J., Zhu, W., Chang, L., Bentler, P. M., and Ernst, T. (2007). Unified structural equation modeling approach for the analysis of multisubject, multivariate functional MRI data. *Human Brain Mapping*, 28(2):85–93. DOI: 10.1002/hbm.20259. http://www3.interscience.wiley.com/cgi-bin/abstract/112634766/.

Kleinschmidt, A., Merboldt, K. D., Hanicke, W., Steinmetz, H., and Frahm, J. (1994). Correlational imaging of thalamocortical coupling in the primary visual pathway of the human brain. *Journal of Cerebral Blood Flow and Metabolism*, 14(6):954–957. PMID: 7929658.

Koch, M. A., Norris, D. G., and Hund-Georgiadis, M. (2002). An investigation of functional and anatomical connectivity using magnetic resonance imaging. *NeuroImage*, 16(1):241–250. http://www.idealibrary.com/links/doi/10.1006/nimg.2002.1076. Assess anatomical connectivity by diffusion-weighted magnetic resonance imaging and functional connectivity by resting state BOLD fMRI (a la Biswal). The functional connectivity showed little correlation for white matter and high correlation among grey matter areas particularly corresponding areas collateral.

Koutsofios, E. and North, S. C. (1996). *Drawing graphs with* dot. AT&T Bell Laboratories, Murray Hill, New Jersey.

Krause, B. J., Horwitz, B., Taylor, J. G., Schmidt, D., Mottaghy, F. M., Herzog, H., Halsband, U., and Muller-Gartner, H. (1999). Network analysis in episodic encoding and retrieval of word-pair associates: a PET study. *European Journal of Neuroscience*, 11(9):3293–3301. PMID: 10510193. This is a network analysis with no Talairach coordinates.

Lee, L., Friston, K. J., and Horwitz, B. (2006). Large-scale neural models and dynamic causal modelling. *NeuroImage*, 30(4):1243–1254. PMID: 16387513.

Lohmann, G. and Bohn, S. (2002). Using replicator dynamics for analyzing fMRI data of the human brain. *IEEE Transactions on Medical Imaging*, 21(5):485–492.

Lowe, M. J. (1999). Functional connectivity with continuous state fMRI assessed with structural equations. *NeuroImage*, 9(6):S197.

Lowe, M. J., Mock, B. J., and Sorenson, J. A. (1998). Functional connectivity in single and multislice echoplanar imaging using resting-state fluctualations. *NeuroImage*, 7(2):119–132. PMID: 9558644. http://linkinghub.elsevier.com/retrieve/pii/S1053811997903153.

Lund, T. E. (2001). fcMRI - mapping functional connectivity or correlating cardiac-induced noise? *Magnetic Resonance in Medicine*, 46(3):628. DOI: 10.1002/mrm.1238.

Maguire, E. A., Mummery, C. J., and Büchel, C. (2000). Patterns of hippocampal-cortical interaction dissociate temporal lobe memory subsystems. *Hippocampus*, 10:475–482. fMRI study.

Mardia, K. V., Kent, J. T., and Bibby, J. M. (1979). *Multivariate Analysis*. Probability and Mathematical Statistics. Academic Press, London. ISBN 0124712525.

McArdle, J. J. and McDonald, R. P. (1984). Some algebraic properties of the reticular action model for moment structures. *British Journal of Mathematical and Statistical Psychology*, 37:234–251. PMID: 6509005.

McIntosh, A. R. (1998). Understanding neural interactions in learning and memory using functional neuroimaging. *Ann. New York Academy of Sci.*, 855:556–571. PMID: 9929651.

McIntosh, A. R. (1999). Mapping cognition to the brain through neural interactions. *Memory*, 7(5–6):523–548. PMID: 10659085.

McIntosh, A. R. (2000). Towards a network theory of cognition. *Neural Network*, 13:861–870.

McIntosh, A. R. and Gonzalez-Lima, F. (1991). Structural modeling of functional neural pathways mapped with 2-deoxyglucose: Effects of acoustic startle habituation on the auditory system. *Brain Research*, 547(2):295–302. PMID: 1884204.

McIntosh, A. R. and Gonzalez-Lima, F. (1992). Structural modeling of functional visual pathways mapped with 2-deoxyglucose: Effects of patterned light and footshock. *Brain Research*, 578(1–2):75–86. PMID: 1511292. ISSN 0006-8993.

McIntosh, A. R. and Gonzalez-Lima, F. (1994a). Network interactions among limbic cortices, basal forebrain, and cerebellum differentiate a tone conditioned as a Pavlovian excitor or inhibitor: fluorodeoxyglucose mapping and covariance structural modeling. *Journal of Neurophysiology*, 72(4):1717–1733. PMID: 7823097.

McIntosh, A. R. and Gonzalez-Lima, F. (1994b). Structural equation modeling and its application to network analysis in functional brain imaging. *Human Brain Mapping*, 2(1 and 2):2–22. ISSN 1065-9471. General introduction to structural equation modeling in functional brain imaging. Examples are given with object and spatial vision in a human PET study and a rat brain study for the geniculocortical circuit.

McIntosh, A. R., Grady, C. L., Ungerleider, L. G., Haxby, J. V., Rapoport, S. I., and Horwitz, B. (1994). Network analysis of cortical visual pathways mapped with PET. *Jornal of Neuroscience*, 14(2):655–666. PMID: 8301356.

McIntosh, A. R. and Lobaugh, N. L. (2004). Partial least squares analysis of neuroimaging data: applications and advances. *NeuroImage*, 23(1):S250–S263. DOI: 10.1016/j.neuroimage.2004.07.020.

McKiernan, K. A., Conant, L. L., Chen, A., and Binder, J. R. (2001). Development and cross-validation of a model of linguistic processing using neural network and path analyses with FMRI data. *NeuroImage*, 13(6):S200. Shortly describes a connection analysis on fMRI data with "path analysis" and an associative neural network in connection with visual implicit language processing.

Mechelli, A., Friston, K. J., Frackowiak, R. S. J., and Price, C. J. (2005). Structural covariance in the human cortex. *The Journal of Neuroscience*, 25(36):8303–8310. DOI: 10.1523/JNEUROSCI.0357-05.2005.

Mechelli, A., Penny, W. D., Price, C. J., Gitelman, D. R., and Friston, K. J. (2002). Effective connectivity and intersubject variability: using a multisubject network to test differences and commonalities. *NeuroImage*, 17(3):1459–1469. PMID: 12414285.

Metter, E. J., Riege, W. H., Kameyama, M., Kuhl, D. E., and Phelps, M. E. (1984a). Cerebral metabolic relationships for selected brain regions in Alzheimer's, Huntington's, and Parkinson's diseases. *Journal of Cerebral Blood Flow and Metabolism*, 4(4):500–506.

Metter, E. J., Riege, W. H., Kuhl, D. E., and Phelps, M. E. (1984b). Cerebral metabolic relationships for selected brain regions in healthy adults. *Journal of Cerebral Blood Flow and Metabolism*, 4(1):1–7. ISSN 0271-678X.

Meyer-Lindenberg, A., Hariri, A. R., Munoz, K. E., Mervis, C. B., Mattay, V. S., colleen A. Morris, and Berman, K. F. (2005). Neural correlates of genetically abnormal social cognition in Williams syndrome. *Nature Neuroscience*, 8(8):991–993. DOI: 10.1038/nn1494.

Meyer-Lindenberg, A., Kohn, P., Mervis, C. B., Kippenhan, J. S., Olsen, R. K., Morris, C. A., and Berman, K. F. (2004). Nerual basis of genetically determined visuospatial construction deficit in Williams syndrome. *Neuron*, 43:623–631. fMRI, voxel-based morphometry and structural equation modeling neuroimaging study.

Moeller, J. R., Strother, S. C., Sidtis, J. J., and Rottenberg, D. A. (1987). Scaled subprofile model: A statistical approach to the analysis of functional patterns in positron emission tomographic data. *Journal of Cerebral Blood Flow and Metabolism*, 7:649–658.

Mopritz, C., Arfanakis, K., Cordes, D., Haughton, V., and Meyerand, M. E. (2000). Connectivity analysis of fMRI activation datasets. *NeuroImage*, 11(5):S575. Cross-correlation with time-series from seed voxels located in rolandic cortex, ventrolateral thalamus and anterior putamen.

Muthén, L. K. and Muthén, B. O. (2006). *Mplus. Statistical Analysis With Latent Variables. User's Guide.* Muthén and Muthén, Los Angeles, California. http://www.statmodel.com/download/usersguide/Mplus%20Users%20Guide%20v41.pdf. Version 4.1.

Nair, H. P. and Gonzalez-Lima, F. (2003). Large-scale networks in learning analyzed with partial least squares. In Sommer, F. T. and Wichert, A., editors, *Exploratory analysis and data modeling in functional neuroimaging*, pages 273–294. MIT Press, Cambridge, MA, USA. ISBN 0262194813.

Neale, M. C., Boker, S. M., Xie, G., and Maes, H. H. (2003). *Mx: Statistical Modeling.* Virginia Institute for Psychiatric and Behavioral Genetics, Virginia Commonwealth University, Richmond, VA, sixth edition. http://www.vipbg.vcu.edu/~vipbg/software/mxmanual.pdf.

Nezafat, R., Shadmehr, R., and Holcomb, H. H. (2001). Long-term adaptation to dynamics of reaching movements: a PET study. *Experimental Brain Research*, 140(1):66–76. PMID: 11500799. http://link.springer-ny.com/link/service/journals/00221/bibs/1140001/11400066.htm.

Nielsen, F. Å., Hansen, L. K., and Strother, S. C. (1998). Canonical ridge analysis with ridge parameter optimization. *NeuroImage*, 7(4, part 2):S758. http://www2.imm.dtu.dk/pubdb/views-/publication_details.php?id=4981. 4th International Conference on Functional Mapping of the Human Brain. June 7–12, 1998, Montreal, Quebec, Canada.

Nyberg, L., McIntosh, A. R., Cabeza, R., Nilsson, L.-G., Houle, S., Habib, R., and Tulving, E. (1996). Network analysis of positron emission tomography regional cerebral blood flow data: ensemble inhibition during episodic memory retrieval. *Journal of Neuroscience*, 16(11):3753–3759. PMID: 8642418. ISSN 0270-6474.

Paulson, O. B. (1970). Regional cerebral blood flow in apoplexy due to occlusion of the middle cerebral artery. *Neurology*, 20(1):63–77. PMID: 5460771.

Paulson, O. B., Lassen, N. A., and Skinhøj, E. (1970). Regional cerebral blood flow in apoplexy without arterial occlusion. *Neurology*, 20(1):125–138. PMID: 5460771.

Penny, W. D., Stephan, K. E., Mechelli, A., and Friston, K. J. (2004). Modelling functional integration: a comparison of structural equation and dynamic causal models. *NeuroImage*, 23(Supplement 1):S264–S274. PMID: 15501096. http://www.fil.ion.ucl.ac.uk/~wpenny/publications/integration.pdf.

Petersson, K. M., Reis, A., Askelof, S., Castro-Caldas, A., and Ingvar, M. (2000). Language processing modulated by literacy: a network analysis of verbal repetition in literate and illiterate subjects. *Journal of Cognitive Neuroscience*, 12(3):364–382. PMID: 10931764.

Rajah, M. N., McIntosh, A. R., and Grady, C. L. (1999). Frontotemporal interactions in face encoding and recognition. *Brain Research. Cognitive Brain Research*, 8(3):259–269. PMID: 10556604.

Sánchez, B. N., Budtz-Jørgensen, E., Ryan, L. M., and Hu, H. (2005). Structural equation models: A review with applications to environmental epidemiology. *Journal of the American Statistical Association*, 100(472):1443–1455. DOI: 10.1198/016214505000001005.

Shimizu, S., Hoyer, P. O., Hyvärinen, A., and Kerminen, A. (2006). A linear nongaussian acyclic model for causal discovery. *Journal of Machine learning Research*, 7:2003–2030. http://www.jmlr.org/papers-/volume7/shimizu06a/shimizu06a.pdf.

Steele, J. D., Meyer, M., and Ebmeier, K. P. (2004). Neural predictive error signal correlates with depressive illness severity in a game paradigm. *NeuroImage*, 23(1):269–280. PMID: 15325374. DOI: 10.1016/j.neuroimage.2004.04.023.

Stein, J. L., Wiedholz, L. M., Weinberg, D., Mattay, V. S., and Meyer-Lindenberg, A. (2006). Automatic construction and stringent validation of path models from human fMRI data. In *Neuroscience*. Society for Neuroscience. #492.10/PP85. A Bullmore-like construction of network models (structural equation models) with minimization by adaptive simulated annealing and split half validation. The title on the poster was "A Validated Network of Effect Amygdala Connectivity During Perceptual Processing of Negative Emotional Stimuli".

Stein, T., Moritz, C., Quigley, M., Cordes, D., Haughton, V., and Meyerand, E. (2000). Functional connectivity in the thalamus and hippocambus studied with functional MR imaging. *AJNR American Journal of Neuroradiology*, 21:1397–1401. http://ntp.neuroscience.wisc.edu/students/student-art/stein21.pdf.

Stephan, K. E., Magnotta, V. A., White, T., Arndt, S., Flaum, M., O'Leary, D. S., and Andreasen, N. C. (2001). Effects of olanzapine on cerebellar functional connectivity in schizophrenia measured by fMRI during a simple motor task. *Psychological Medicine*, 31(6):1065–1078. PMID: 11513374. http://journals.cambridge.org/abstract_S0033291701004330.

Sychra, J. J., Bandettini, P. A., Bhattacharya, N., and Lin, Q. (1994). Synthetic images by subspace transform. I. principal components images and related filters. *Medical Physics*, 21(2):193–201. PMID: 8177152.

Taylor, J. G., Krause, B., Shah, N. J., Horwitz, B., and Mueller-Gaertner, H. W. (2000). On the relation between brain imagings and brain neural networks. *Human Brain Mapping*, 9(3):165–182. PMID: 10739367.

Worsley, K. J., Cao, J., Paus, T., Petrides, M., and Evans, A. C. (1998a). Applications of random field theory to functional connectivity. *Human Brain Mapping*, 6:364–367. http://www.math.mcgill.ca/~keith/bm97/bm97.abstract.html.

Worsley, K. J., Cao, J., Paus, T., Petrides, M., and Evans, A. C. (1998b). Detecting functional connectivity by threshlding correlation random fields. *NeuroImage*, 7:S36. http://www.math.mcgill.ca/~keith/HBM98/HBM98.ps. Short description of determination of functional connectivity by examining the cross-correlation between voxels and determing a threshold setting from random field theory. The method is exemplified on a positron emission tomography data set.

Worsley, K. J., Charil, A., Lerch, J., and Evans, A. C. (2005a). Connectivity of anatomical and functional MRI data. In *International Joint Conference on Neural Networks, July 31-August 4, 2005, Montreal, Quebec, Canada*. http://www.math.mcgill.ca/keith/oury/oury2.pdf.

Worsley, K. J., Chen, J.-I., Lerch, J., and Evans, A. C. (2005b). Comparing connectivity via thresholding correlations and SVD. *Philosophical Transactions of the Royal Society*, 360:913–920.

Xiong, J., Parsons, L. M., Gao, J.-H., and Fox, P. T. (1999). Interregional connectivity to primary motor cortex revealed using MRI resting state images. *Human Brain Mapping*, 8(2-3):151–156. http://www3.interscience.wiley.com/cgi-bin/fulltext/66000621/PDFSTART.

Index